Supplementary Information

Self-Doped p-n Junctions in Two-Dimensional In_2X_3 van der Waals Materials

Rui Peng[†], Yandong Ma[†, *], Shuai Zhang[†], Baibiao Huang[†], Liangzhi Kou[‡] and Ying Dai[†, *]

[†] School of Physics, State Key Laboratory of Crystal Materials, Shandong University, Shandanan Street 27, Jinan 250100, China

[‡] School of Chemistry, Physics and Mechanical Engineering Faculty, Queensland University of Technology, Garden Point Campus, QLD 4001, Brisbane, Australia

*Email: yandong.ma@sdu.edu.cn (Y.M.); daiy60@sina.com (Y.D.)

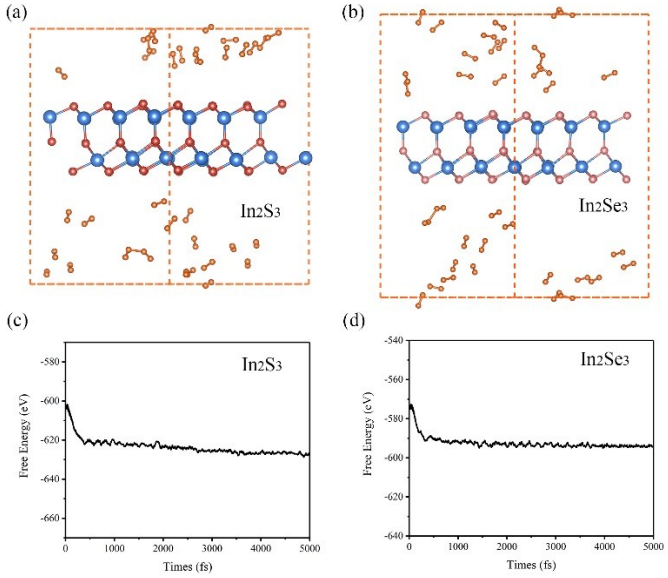

Fig. S1 Structure snapshots of (a) SL In_2S_3-O_2 and (b) SL In_2Se_3-O_2 for AIMD simulations at 300 K. Variations of the free energy of (c) SL In_2S_3-O_2 and (d) SL In_2Se_3-O_2 during AIMD simulations at 300 K.

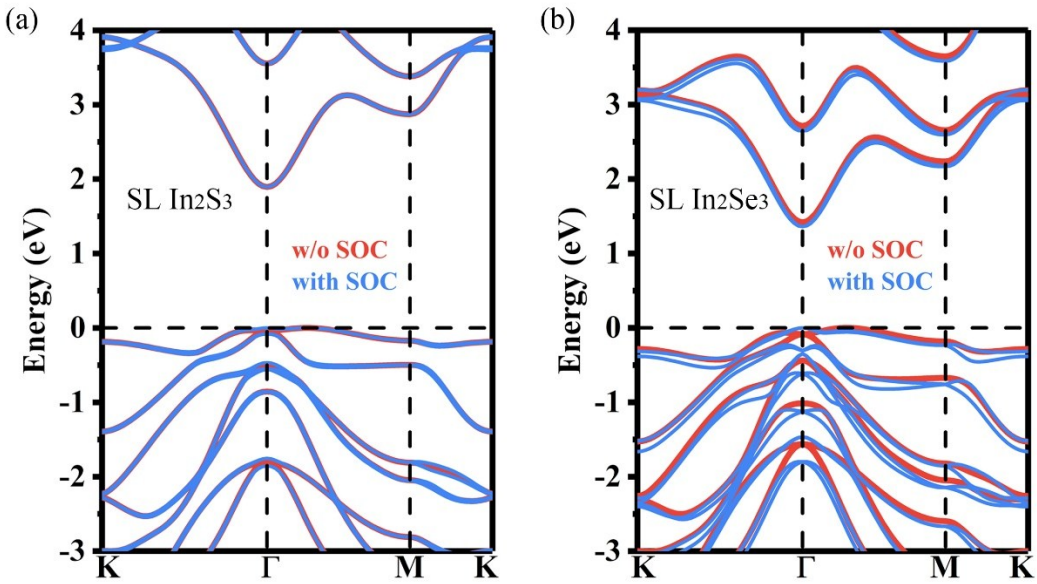

Fig. S2 Band structures of SL In_2X_3 without and with SOC. The Fermi level is set to 0 eV.

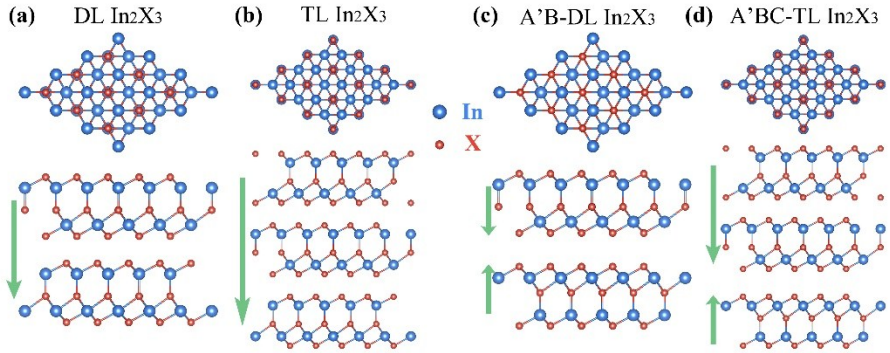

Fig. S3 Top and side views of the crystal structures of (a) DL In_2X_3, (b) TL In_2X_3, (c) A'B-DL In_2X_3 and (d) A'BC-TL In_2X_3. The orientation of intrinsic dipole is represented by green arrows.

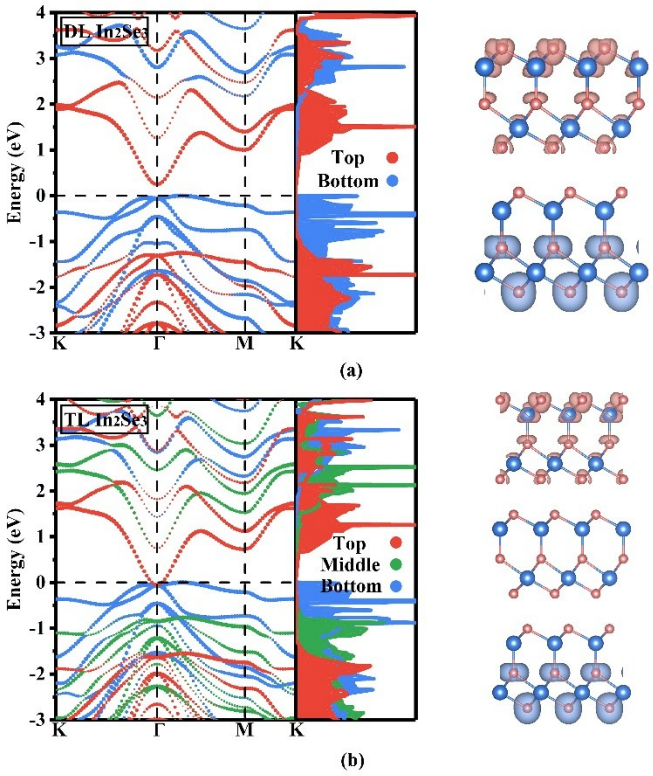

Fig. S4 Fat band structures, DOS, and partial charge density of CBM and VBM based on HSE06 level for (a) DL In_2Se_3 and (b) TL In_2Se_3. The Fermi level is set to 0 eV. Red (blue) regions in the right panels represent the band decomposed charge density for CBM (VBM). The isosurface value is set to 0.04 e $Å^{-3}$.

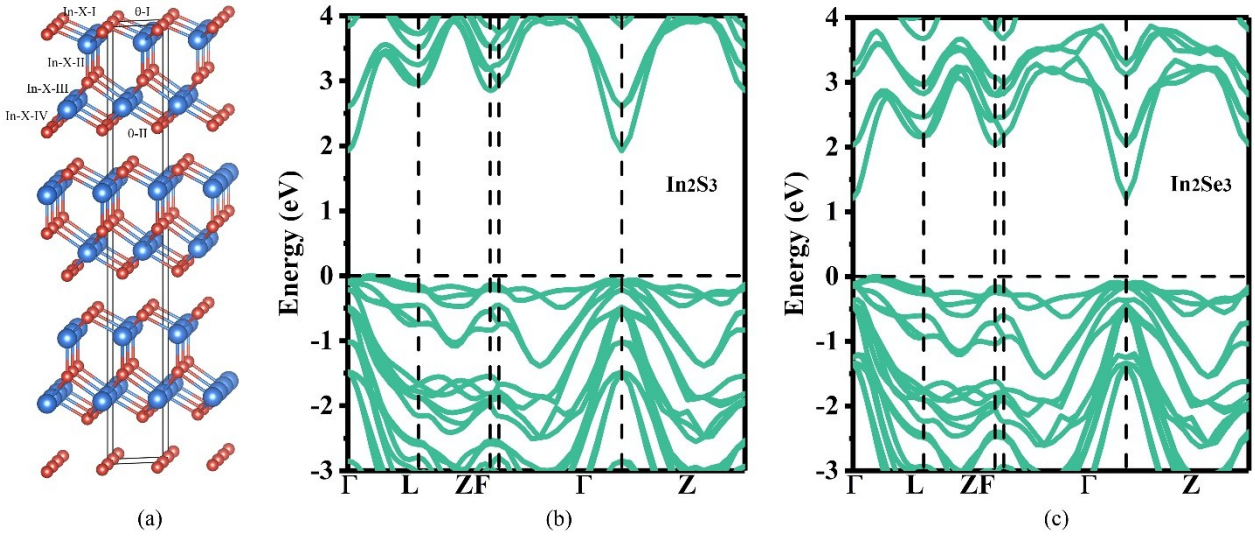

Fig. S5 (a) Crystal structure of bulk In_2X_3. Band structure of (b) bulk In_2S_3 and (c) bulk In_2Se_3.

Table S1 The lattice constants a (Å) calculated by DFT-D2, optPBE-vdW and SCAN.

	DFT-D2	optPBE-vdW	SCAN
DL In_2S_3	3.85	3.93	3.89
DL In_2Se_3	4.00	4.09	4.06
TL In_2S_3	3.85	3.93	3.89
TL In_2Se_3	4.00	4.09	4.06

Table S2 The bond length and angle of SL, DL, TL and bulk In_2X_3.

	In_2S_3				In_2Se_3			
	SL	DL	TL	Bulk	SL	DL	TL	Bulk
In-X-I (Å)	2.68	2.65	2.65	2.64	2.55	2.53	2.53	2.51
In-X-II (Å)	2.56	2.53	2.54	2.55	2.43	2.41	2.42	2.43
In-X-III (Å)	2.90	2.86	2.85	2.84	2.79	2.75	2.75	2.73
In-X-IV (Å)	2.72	2.69	2.69	2.70	2.58	2.55	2.56	2.57
θ-I (°)	99.90	97.80	97.83	98.76	100.99	99.01	99.17	100.39
θ-II (°)	98.18	96.08	95.99	95.87	99.55	97.59	97.44	97.34

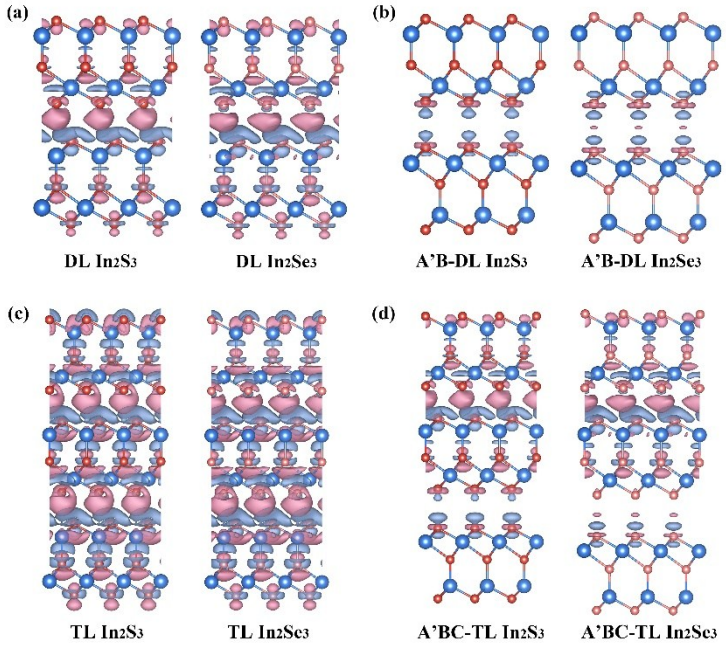

Fig. S6 Charge density differences of DL In_2X_3 and individual In_2X_3 layers for (a) DL In_2X_3 and (b) A'B-DL In_2X_3. Charge density differences of TL In_2X_3 and individual In_2X_3 layers for (c) TL In_2X_3

and (d) A'BC-TL In_2X_3. The Red and blue regions indicate the accumulation and depletion of electrons, respectively. The isosurface value is set to 0.001 e $Å^{-3}$.

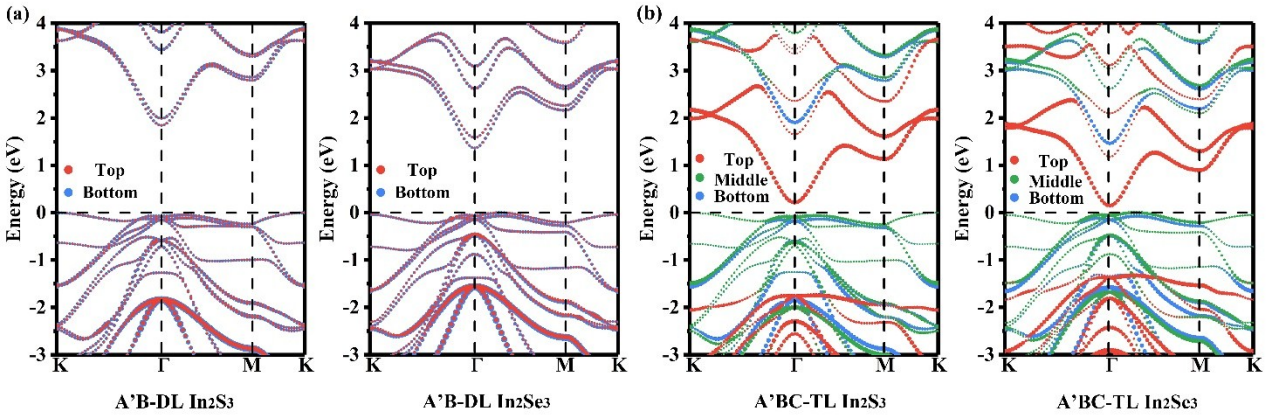

Fig. S7 Fat band structures based on HSE06 level of (a) A'B-DL In_2X_3 and (b) A'BC-TL In_2X_3. The Fermi level is set to 0 eV.

Note 1

In order to simulate In_2S_3/G and G/In_2S_3, the 3 * 3 supercell of graphene is used to match the 2 * 2 supercell of In_2S_3. As for In_2Se_3/G and G/In_2Se_3, the $\sqrt{3}$* $\sqrt{3}$ supercell of graphene is used to match the 1 * 1 supercell of In_2Se_3. The induced lattice mismatch is 3.8% and 3.9%, respectively. The binding energy between graphene and SL In_2X_3 is calculated according to the below expression:

$$E_b = (E_{het} - E_{In2X3} - E_G)/N_C,$$

where E_{het}, E_{In2X3}, and E_G are the total energies of the heterostructures (In_2X_3/G and G/In_2X_3), SL In_2X_3, and graphene, respectively; N_C is the number of carbon atoms. The calculated binding energies for In_2S_3/G (In_2Se_3/G) and G/In_2S_3 (G/In_2Se_3) are 0.26 (0.18) and 0.32 (0.17) eV, respectively, indicating that weak interlayer vdW interactions. The interlayer spacing for G/In_2S_3 and In_2S_3/G are found to be 3.36 and 3.42 Å, respectively. We hypothetically change the interlayer spacing of In_2S_3/G from 3.42 to 3.36 Å and find that its band structure is slightly changed (see **Fig. S11**). The interlayer spacing for G/In_2Se_3 and In_2Se_3/G are both 3.38 Å.

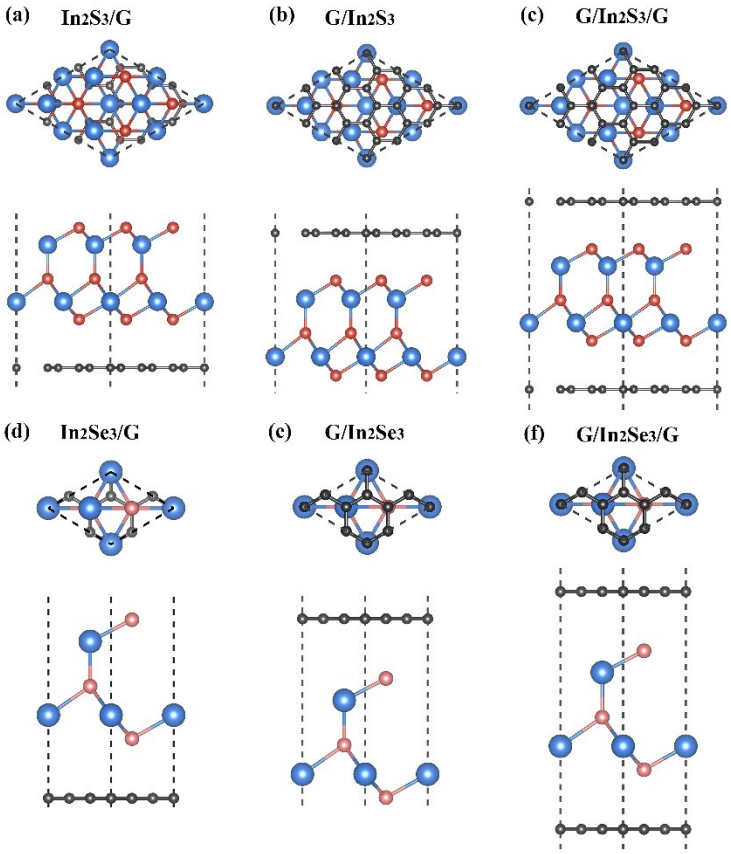

Fig. S8 Top and side views of the crystal structures of (a) In_2S_3/G, (b) G/In_2S_3, (c) G/In_2S_3/G, (d) In_2Se_3/G, (e) G/In_2Se_3, and (f) G/In_2Se_3/G.

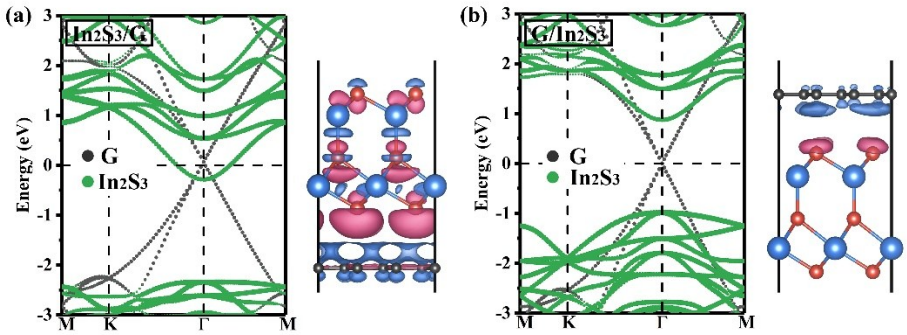

Fig. S9 Fat band structures based on HSE06 level and charge density differences of (a) In_2S_3/G and (b) G/In_2S_3. The Fermi level is set to 0 eV. The Red and blue regions in the right panels of (a, b) indicate the accumulation and depletion of electrons, respectively. The isosurface value is set to 0.001 e Å^{-3}.

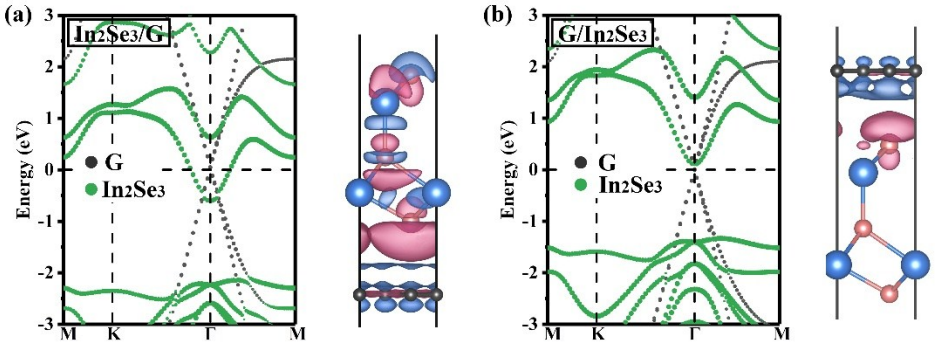

Fig. S10 Fat band structures based on HSE06 level and charge density differences of (a) In_2Se_3/G and (b) G/In_2Se_3. The Fermi level is set to 0 eV. The Red and blue regions in the right panels of (a, b) indicate the accumulation and depletion of electrons, respectively. The isosurface value is set to 0.001 e Å^{-3}.

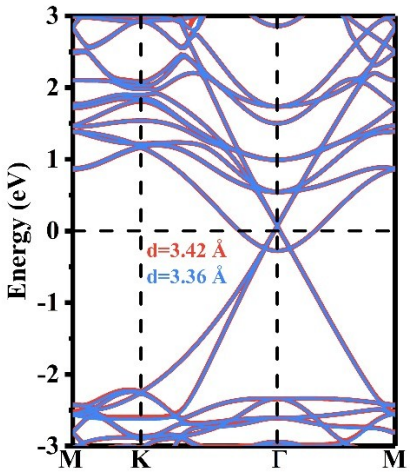

Fig. S11 Band structure of In_2Se_3/G with an interlayer distance of 3.42 Å and 3.36 Å.

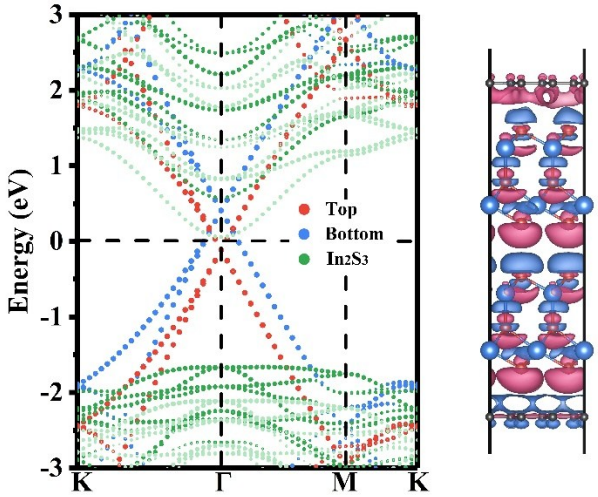

Fig. S12 Fat band structure based on HSE06 level and charge density difference of G/DL In_2S_3/G. The Fermi level is set to 0 eV. The Red and blue regions in the right panel indicate the accumulation and depletion of electrons, respectively. The isosurface value is set to 0.001 e Å^{-3}.

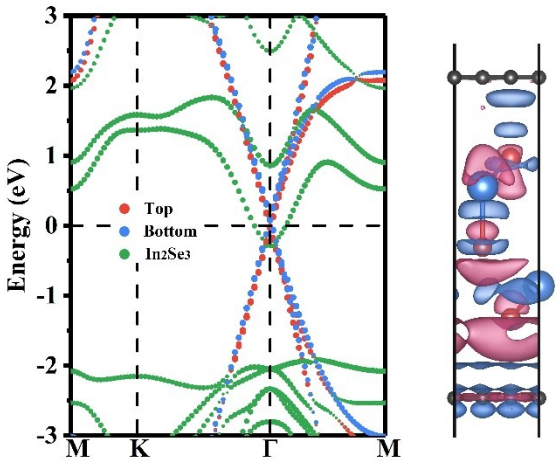

Fig. S13 Fat band structure based on HSE06 level and charge density difference of G/In_2Se_3/G. The Fermi level is set to 0 eV. The Red and blue regions in the right panel indicate the accumulation and depletion of electrons, respectively. The isosurface value is set to 0.001 e $Å^{-3}$.

Note 2

The heterostructure of G/In_2Se_3/G is constructed. Regretfully, the Dirac points of two graphene layers are almost undisguisable. From the charge density difference, we can see that there are no electrons around the top-layer graphene, implying that the top-layer graphene is not p-doped. Additionally, the CBM of SL In_2Se_3 cross the fermi level, which is not desirable for practical application.